Received: 3 July 2020 | Revised: 15 August 2020 | Accepted: 26 August 2020

DOI: 10.1111/apha.13553

REGULAR PAPER

ACTA PHYSIOLOGICA

The body region specificity in murine models of muscle regeneration and atrophy

Kiyoshi Yoshioka | **Yasuo Kitajima** | **Daiki Seko** | **Yoshifumi Tsuchiya** | **Yusuke Ono**

Department of Muscle Development and Regeneration, Institute of Molecular Embryology and Genetics, Kumamoto University, Kumamoto, Japan

Correspondence
Yusuke Ono, Department of Muscle Development and Regeneration, Institute of Molecular Embryology and Genetics, Kumamoto University, 2-2-1 Honjo, Kumamoto 860-0811, Japan.
Email: ono-y@kumamoto-u.ac.jp

Funding information
Japan Society for the Promotion of Science; Takeda Medical Research Foundation; Japan Agency for Medical Research and Development

Abstract

Aim: Skeletal muscles are distributed throughout the body, presenting a variety of sizes, shapes and functions. Here, we examined whether muscle regeneration and atrophy occurred homogeneously throughout the body in mouse models.

Methods: Acute muscle regeneration was induced by a single intramuscular injection of cardiotoxin in adult mice. Chronic muscle regeneration was assessed in *mdx* mice. Muscle atrophy in different muscles was evaluated by cancer cachexia, ageing and castration mouse models.

Results: We found that, in the cardiotoxin-injected acute muscle injury model, head muscles slowly regenerated, while limb muscles exhibited a rapid regeneration and even overgrowth. This overgrowth was also observed in limb muscles alone (but not in head muscles) in *mdx* mice as chronic injury models. We described the body region–specific decline in the muscle mass in muscle atrophy models: cancer cachexia-induced, aged and castrated mice. The positional identities, including gene expression profiles and hormone sensitivity, were robustly preserved in the ectopically engrafted satellite cell-derived muscles in the castrated model.

Conclusion: Our results indicate that positional identities in muscles should be considered for the development of efficient regenerative therapies for muscle weakness, such as muscular dystrophy and age-related sarcopenia.

KEYWORDS

ageing, cancer cachexia, castration, heterogeneity, muscle atrophy, positional memory, skeletal muscle

1 | INTRODUCTION

Skeletal muscle is the contractile tissue that is distributed throughout the body. Its size and shape are anatomically and physiologically diverse, presenting a variety of functions such as movement, respiration, articulation, facial expression and mastication. It is well known that muscle fibre-type composition varies from a fast twitch to a slow twitch, where contraction proteins, energy metabolism and mitochondrial contents are different among the fibre types.[1] The differences in fibre types also influence the effects of ageing and cancer cachexia in muscles.[1,2]

Adult skeletal muscle regenerates after an injury, and this regenerative capacity relies on the resident muscle tissue stem cells, namely, the satellite cells.[3] However, a satellite cell dysfunction is observed in muscle diseases,[4,5] such as muscular dystrophy, where muscle degenerative and regenerative cycles are repeated, gradually resulting in a regeneration

failure. Clinical observations have provided evidence of the distribution of region-specific predominant muscle pathology in different types of muscular dystrophies.[6] These observations indicate that muscle regeneration is regulated in a body region–dependent manner. Studies revealed that satellite cells constitute a functionally heterogeneous population in different muscles, depending on the fibre types as well as the embryonic origins.[7–16] Satellite cells in the pharyngeal muscle of the head constitutively proliferate and contribute to a myonuclear turnover under basal conditions, while this phenomenon is rarely observed in uninjured limb muscles.[17] Thus, the characteristics of certain muscles are not always applicable to other muscles. However, little attention has been paid to differences in the body region–specific properties in skeletal muscles, especially on head muscles originated mainly from the cranial mesoderm.[18] Here, we examined how muscles were regionally and specifically affected in mouse models of muscle regeneration and atrophy.

2 | MATERIALS AND METHODS

2.1 | Animals and in vivo experiments

The Experimental Animal Care and Use Committee of the Kumamoto University approved the animal experiments (Ref. No. A30-098). Wild-type (WT, C57/BL6J) and *mdx* mice were obtained from CREA Japan, Inc (Tokyo, Japan).

For muscle injury, mice were anaesthetized, and the hair on the lower jaw and lower leg areas was removed with a depilatory cream (Kracie, Tokyo, Japan). The facial nerve was percutaneously identified to avoid needle damage. To induce muscle injury in anaesthetized mice, 50 μl and 40 μL of 10 μmol/L cardiotoxin (CTX) were injected into the tibialis anterior (TA) and the masseter (MAS) muscles respectively. CTX-injected and non-injected (intact) muscles were harvested for transverse sectioning and immunostaining.

In the cancer cachexia model, mice were injected subcutaneously in the lower back with 1×10^6 cells of the Lewis lung carcinoma (LLC) cell line in PBS. Control mice were injected with PBS alone. The mice were sacrificed 4 weeks after the injections. Castration was performed in 3-month-old male mice under anaesthesia. The skin of the scrotum was incised and the testicles were removed. Sham-operated mice were used as controls. To measure the diameter of the urethral sphincter (US), the urethral-specific muscle composed of urethral wall described as the peri-urethral sphincter was used.

For cell transplantation, Dmd^{mdx}/Y homozygous male *mdx* and Dmd^{mdx}/Dmd^{mdx} homozygous female *mdx* mice were used as recipient mice. These mice were anaesthetized and their hind limbs were locally exposed to 18 Gy of γ-radiation to eliminate the endogenous satellite cells.[19] CTX was injected into the TA muscle immediately after the irradiation, and 1×10^4 YFP^+ satellite cells sorted from the hind-limb muscles (TA, EDL, GAS, PLA, and SOL) or the perineal muscles (LA and BUL) of *Pax7-YFP* knock-in mice[20] using a FACS Aria II flow cytometer (BD Immunocytometry Systems, CA) were engrafted into the TA muscles of *mdx* mice as per a previously described method.[20]

2.2 | Immunostaining and imaging

Immunohistochemistry of muscle cross-sections was performed as per a previously described method.[21] Samples were cross-sectioned at the maximum bulge region of each muscle. Briefly, samples were incubated with primary antibodies at 4°C overnight following fixation in 2%-4% paraformaldehyde and blocked/permeabilized in PBS containing 0.3% TritonX-100 and 5% goat serum for 30 minutes, at room temperature. All immunostaining samples were visualized using appropriate species-specific Alexa Fluor 488 and/or 546 fluorescence-conjugated secondary antibodies (Thermo Fisher Scientific, Waltham, MA). Mounting medium containing 4,6-diamidino-2-phenylindole (DAPI) was used for nuclear staining (Nacalai Tesque, Kyoto, Japan). Samples were viewed on an Olympus fluorescence microscope IX83 (Olympus) or BZ-X700 (Keyence). Immunostaining for laminin or haematoxylin-eosin staining was used to measure the cross-sectional area (CSA) of myofibers, and CSA was quantified from at least 300 individual myofibers using Image-J (NIH).

For myofiber diameter measurements, individual myofibers were isolated from the extensor digitorum longus (EDL) and the urethral sphincter (US) muscles by digestion with type I collagenase as per a previously described method.[21] Neuromuscular junctions were visualized by staining with α-Bungarotoxin to identify the longitudinal centre of individual myofibers. The diameters of isolated individual myofibers are not completely uniform through myofibers. To avoid intentional measurements, the diameter of individual myofibers was determined as an average from measurements of two ends of a neuromuscular junction.

2.3 | Real-time PCR

Total RNA was isolated with Isogen II (Nippon Gene) and cDNA was synthesized with the ReverTra Ace kit with genomic DNA remover (Toyobo). Real-time PCR was performed with the Thunderbird SYBR quantitative PCR (qPCR) mix (Toyobo) and the CFX96 Touch real-time PCR detection system (Bio-Rad). The expression levels of selected genes were quantified based on the standard curve method, and the values were normalized with the TATA box binding protein (TBP). Primer sequences used are as follows: TBP [forward (F) 5′–CAGATGTGCGTCAGGCGTTC–3′

and reverse (R) 5′–TAGTGATGCTGGGCACTGCG–3′]; MuRF-1 [F 5′–TGATTCTCGATGGAAACGCTATGG–3′ and R 5′–ATTCGCAGCCTGGAAGATGTC–3′]; Atrogin-1 [F 5′–GACAAAGGGCAGCTGGATTGG–3′ and R 5′–TCAGTGCCCTTCCAGGAGAGA–3′]; Myostatin [F 5′–ACCAGGAGAAGATGGGCTGAATC–3′ and R 5′–GGGATTCCGTGGAGTGCTCA–3′]; Androgen receptor (AR) [F 5′–CAGGAGGAAGGAGAAAACTCCA–3′ and R 5′–ATTGACAAGGCAGCAAAGGAATC–3′]; zinc finger MYND domain-containing protein 17 (Zmynd17) [F 5′–TAGGGCTTAACAGGCACTGGTCCCC–3′ and R 5′–TTCTTGTGCTTTCGCCGCCGTG–3′].

2.4 | Statistical analysis

Statistical analysis was performed using GraphPad Prism 8 (GraphPad Software, San Diego, CA). For statistical comparisons of two conditions, the Student's *t*-test was used. For comparisons of more than two groups, the data were analysed with one-way or two-way ANOVA according to the experimental design followed by the Sidak's multiple comparison test. $P < 0.05$ were considered statistically significant. *n.s.* indicates data that are not statistically significant.

3 | RESULTS

3.1 | Regional-specific phenotypes during muscle regeneration

We first determined how adult muscle regeneration differed between the head and limb muscles. Muscle regeneration was induced by cardiotoxin (CTX) injection into both MAS and TA in mice, who were killed 2, 4, 8 and 40 weeks after injury (Figure 1A). We found that TA efficiently regenerated 2 weeks after injury (Figure 1B). The injured TA muscle of the hind limbs showed a gradual overgrowth: muscle

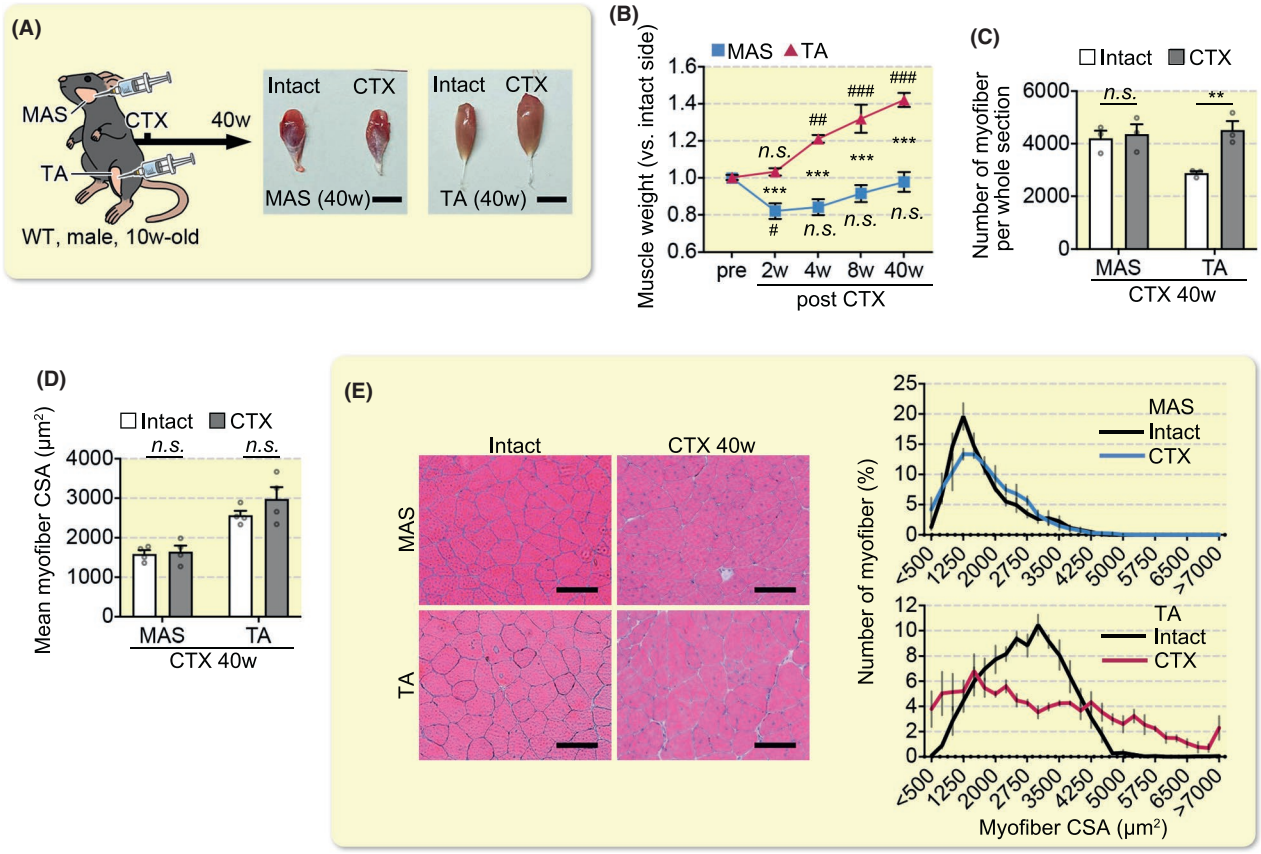

FIGURE 1 Regional specificity in muscle regeneration. (A–E) Muscle regeneration was induced by cardiotoxin (CTX) injection into the masseter (MAS) and the tibialis anterior (TA) muscles of adult male mice. (A) Illustration of the experiment and representative images of muscle tissues 40 weeks after a CTX injection. Scale bars, 5 mm. (B) Time course of regenerating muscle weight change normalized to that of intact muscles (n = 4 mice, $^{\#}P < .05$, $^{\#\#}P < .01$, $^{\#\#\#}P < .001$, intact vs. CTX. $^{***}P < .001$, MAS vs. TA). (C) Number of myofibers per whole muscle tissue section 40 weeks post-injury (n = 3 mice, $^{**}P < .01$). (D) Mean cross-sectional area (CSA) of intact (CTX non-injected side) or centrally nucleated (CTX-injected side) myofibers (n = 4 mice). (E) CSA distribution of MAS and TA at 40 weeks post-injury (n = 4 mice). Scale bars, 100 μm. - Data represent mean ± SEM. All error bars show the standard error of the mean (SEM)

weight and the number of myofibers significantly increased 40 weeks after injury (Figure 1B and C). In the injured head MAS muscle, muscle mass, CSA of regenerating myofibers and the number of myofibers fully returned to basal (intact) levels without overgrowth 40 weeks post-injury (Figure 1A–E). The CSA distribution of the regenerated muscles also differed between the MAS and TA muscles.

We further examined muscle regeneration in the dystrophin-deficient *mdx* mice, a Duchenne muscular dystrophy (DMD) model, in which muscles repeatedly undergo chronic degeneration and regeneration cycles. Although the *mdx* mouse line does not display the severe pathology characterized in human DMD patients, probably caused by the compensatory upregulation of utrophin, an autosomal homologue of dystrophin and longer telomeres in satellite cells,[22] it is useful to evaluate muscle regeneration throughout the body. Consistent with the CTX-induced acute injury models, overgrowth alterations of the limb muscles (but not head muscles) were observed in the *mdx* mice (Figure 2A–E).

3.2 | Effects of cancer cachexia, ageing and sex hormone reduction on different muscles

Afterwards, we determined whether muscle atrophy occurred similarly in different muscles. To induce muscle atrophy, a cancer cachexia-induced muscle atrophy model was established by a subcutaneous injection of 1×10^6 cells of the Lewis lung carcinoma (LLC) line into the lower back region of C57BL6 mice (Figure 3A and B). Mice were killed, and muscle weights were determined 4 weeks after an LLC injection. The weight and CSA of limb muscles, with the exception of the slow-fibre–rich soleus (SOL) muscle, had decreased in the cancer cachexia-induced mice, whereas the MAS and digastric (DIG) muscles of the head were unaffected (Figure 3C and D). Consistent with these results, the muscle atrophy-related genes *MuRF-1*, *Atrogin-1* and *Myostatin*[23,24] were upregulated in atrophic limb muscles but not in the MAS head muscle under cancer cachexia condition (Figure 3E).

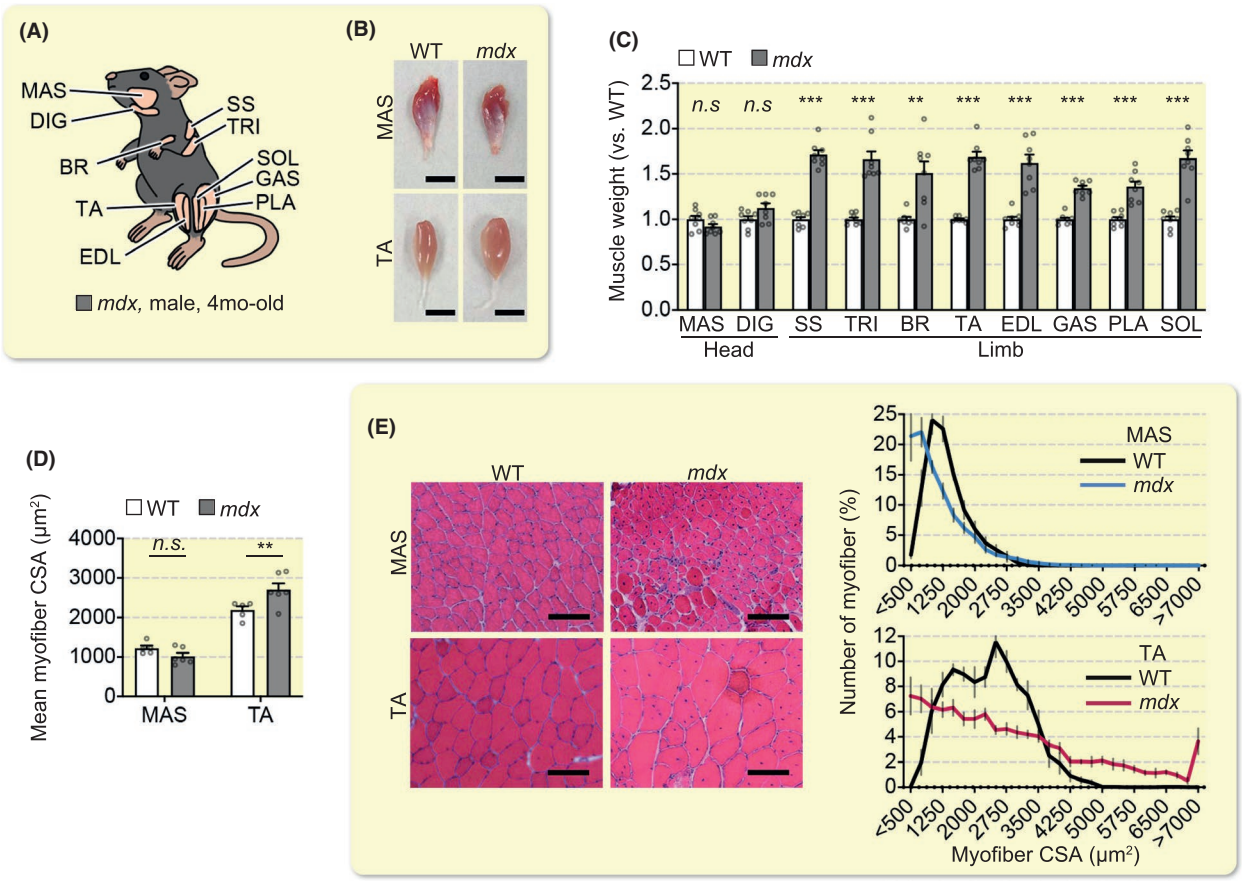

FIGURE 2 Region-specific muscle regeneration in *mdx* mice. (A) Illustration of muscles. SS, supraspinatus; TRI, triceps brachii; BR, brachioradialis; GAS, gastrocnemius; PLA, plantaris; SOL, soleus. (B) Representative images of MAS and TA tissues in wild-type (WT) and *mdx* mice. Scale bars, 5 mm. (C) Muscle weights in *mdx* mice normalized to those in WT mice (WT; n = 8 mice, *mdx*; n = 8 mice). (D) Mean CSA of regenerative myofibers (WT; n = 5 mice, *mdx*; n = 6 mice). (E) CSA distribution of MAS and TA (WT; n = 5, *mdx*; n = 6). Scale bars, 100 μm. Data represent mean ± SEM. All error bars show the standard error of the mean (SEM). $^{**}P < .01$, $^{***}P < .001$. MAS, masseter; DIG, digastric; SS, supraspinatus; TRI, triceps brachii; BR, brachioradialis; TA, tibialis anterior; EDL, extensor digitorum longus; GAS, gastrocnemius; PLA, plantaris; SOL, soleus

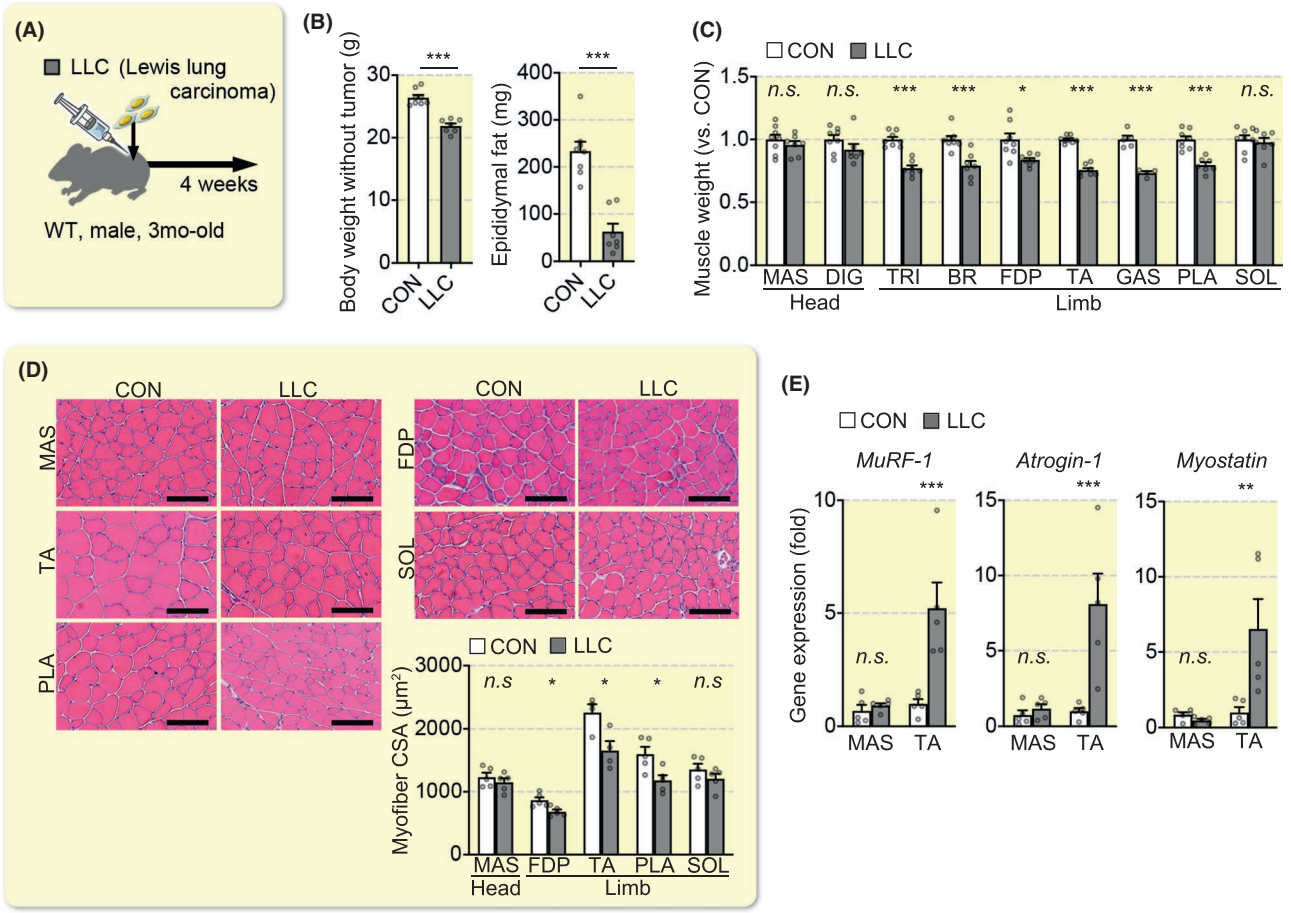

FIGURE 3 Region-specific phenotypes in cancer cachexia. (A) Cancer cachexia was induced by an LLC injection to induce systemic muscle atrophy. (B) Body weight and epididymal fat were weighed (CON; n = 5 mice, LLC; n = 5 mice). (C) Muscle weight (LLC/ CON) at 4 weeks following an LLC injection (CON; n = 8 mice, LLC; n = 7 mice). FDP: flexor digitorum profundus. (D) Representative images of HE-stained muscle tissue sections. Mean myofiber CSA (MAS, FDP, PLA and SOL; n = 5 mice, TA; n = 4 mice). Scale bars, 100 μm. (E) Expression of the atrophy-related genes in MAS and TA (n = 5 mice each). All error bars show the SEM. $*P < .05$, $**P < .01$, $***P < .001$. MAS, masseter; DIG; TRI, triceps brachii; BR, brachioradialis; FDP, flexor digitorum profundus; TA, tibialis anterior; GAS, gastrocnemius; PLA, plantaris; SOL, soleus

Given that muscle atrophic responses in limb muscles were distinct from head muscles in cancer cachexia, we proceeded to investigate the impact of ageing and sex hormone depletion on muscles. Muscle weight and CSA of all limb muscles were remarkably lower in 27-month-old mice compared to 4-month-old mice, whereas head muscles remained unchanged (Figure 4A–C). Region-specific muscle atrophy was also observed in castrated mouse models, where androgen levels were reduced; the levator ani (LA), bulbospongiosus (BUL) and US muscles were significantly reduced, as reported in previous studies[25-27], whereas the head and limb muscle masses remained unaltered after 2 weeks of castration (Figure 5A–E). These findings indicate that perineal muscles are more sensitive to an androgen reduction compared to the sensitivity in the head and limb muscles.

We next examined how robustly the body region identities were maintained. Satellite cells were freshly isolated from the hind limb or perineal muscles of *Pax7-YFP* knock-in male mice and then transplanted into the irradiated and CTX-injected TA muscles of male or female *mdx* mice (Figure 6A). We used *mdx* mice as the recipients because the donor-derived regenerating myofibers would be more easily visible by immunostaining for dystrophin. *mdx* mice were killed for analysis 3 weeks after transplantation. We have recently reported that Zmynd17 is a regulator of the muscle mitochondrial quality, and its expression pattern varies in muscles.[28,29] Since AR and Zmynd17 genes were highly expressed in perineal muscles compared to the expression in the limb muscles (Figure 6B), we used these gene sets as perineal markers. We showed that engrafted satellite cell-derived muscles maintained the gene expression profiles based on anatomical origins in the limb host muscles (Figure 6B and C).

To further examine whether perineal satellite cell-derived muscles also maintained a sensitivity to the reduced androgen levels in ectopic sites, satellite cells were isolated from the perineal muscle in *Pax7-YFP* knock-in male mice as a donor and transplanted into the TA muscles of *mdx* male, castrated *mdx* male or *mdx* female mice. Hind-limb muscle-derived

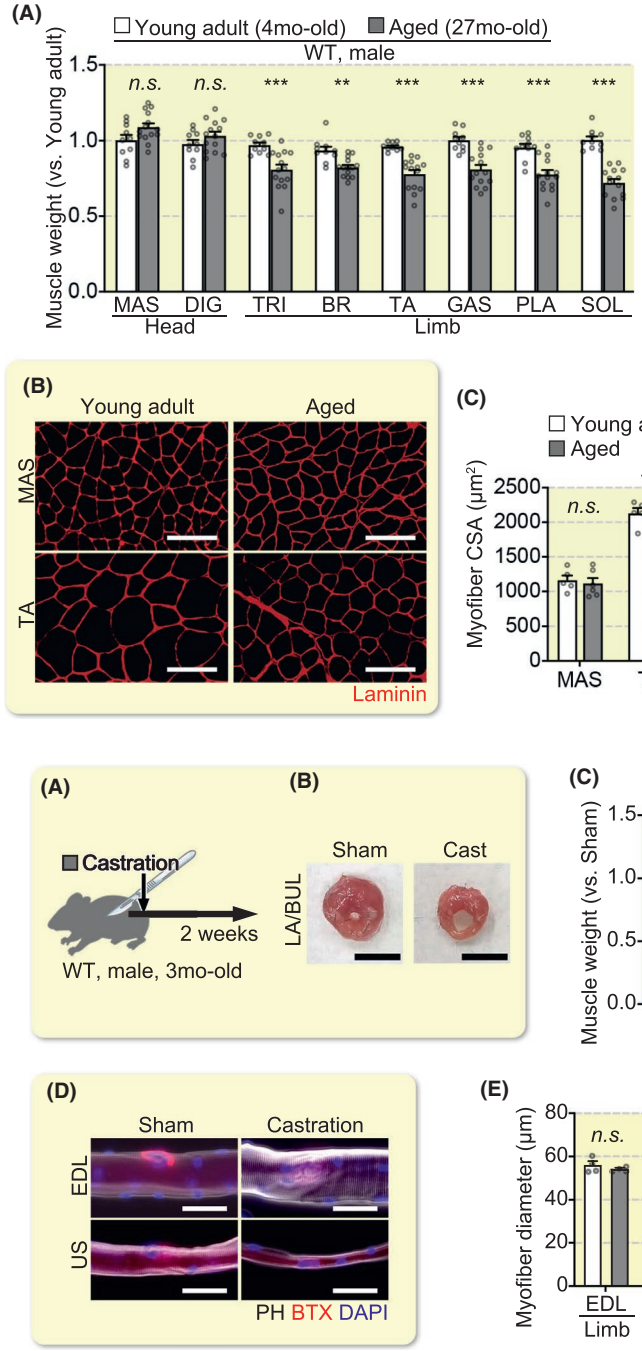

FIGURE 4 Impact of ageing on head and limb muscles. (A) Muscle weight ratio (young adult; n = 10 mice, aged; n = 13 mice). (B) Representative immunohistochemical images of MAS and TA tissue sections stained for laminin. (C) Mean myofiber CSA (young adult; n = 5 mice, aged; n = 6 mice). Scale bars, 100 μm. All error bars show the SEM. $^{**}P < .01$, $^{***}P < .001$. MAS, masseter; DIG; TRI, triceps brachii; BR, brachioradialis; TA, tibialis anterior; GAS, gastrocnemius; PLA, plantaris; SOL, soleus

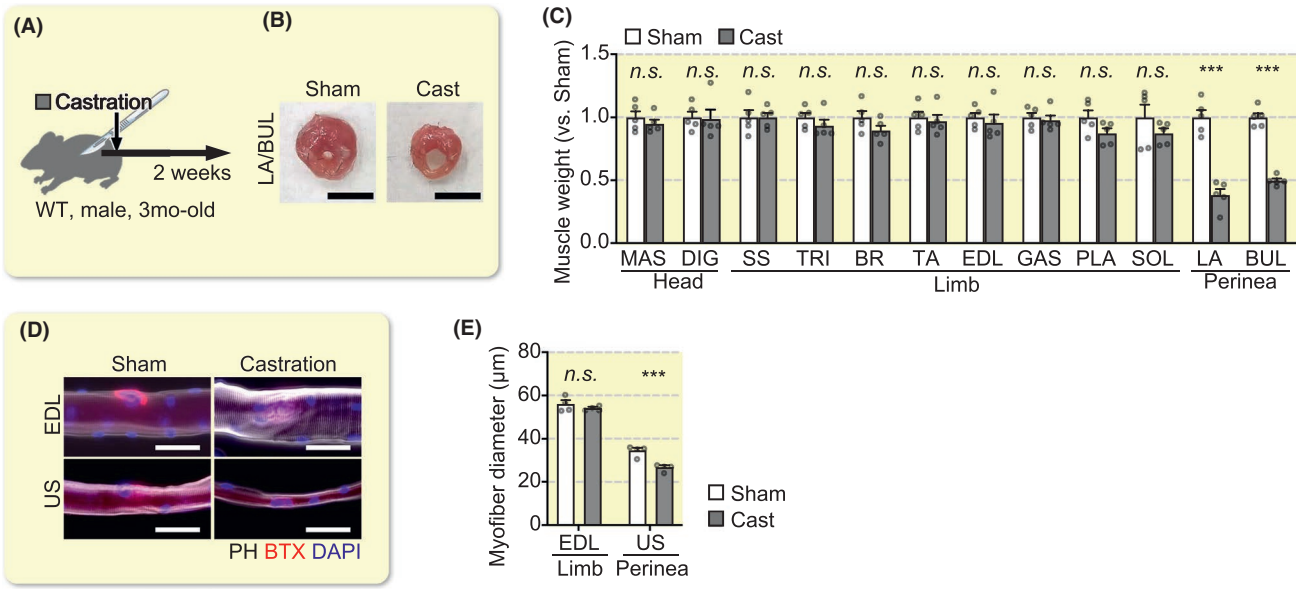

FIGURE 5 Region-specific effects of castration on muscles. (A) Castration was conducted using an androgen insufficient model. (B) Representative muscle tissue images of the LA and BUL. (C) Muscle weight ratio (sham/castration) 2 weeks after the operation (n = 5 mice each). (D) Representative phase-contrast images of individual myofibers isolated from EDL and US. (E) The diameter of individual myofibers (n = 4 mice each, 30 myofibers were counted per mouse). Scale bars, 50 μm. All error bars show the SEM. $^{*}P < .05$, $^{**}P < .01$, $^{***}P < .001$. MAS, masseter; DIG, digastric; SS, supraspinatus; TRI, triceps brachii; BR, brachioradialis; TA, tibialis anterior; EDL, extensor digitorum longus; GAS, gastrocnemius; PLA, plantaris; SOL, soleus; LA, levator ani; BUL, bulbospongiosus; US, urethral sphincter

satellite cells were transplanted into the TA muscles as a control. Immunohistochemical analysis showed that perineal satellite cells gave rise to significantly smaller regenerative myofibers in both castrated male and female *mdx* mice, compared to those in the male *mdx* mice (Figure 6D and E). We also confirmed that perineal satellite cell-derived regenerated muscles were more severely affected by an androgen reduction than the effects observed in the hind-limb satellite cell-derived muscles (Figure 6D and E). Taken together, our findings indicate that muscle atrophy occurs in a body region– and disease model-specific manner, and positional identities in satellite cell-derived muscles are preserved even in the ectopic sites.

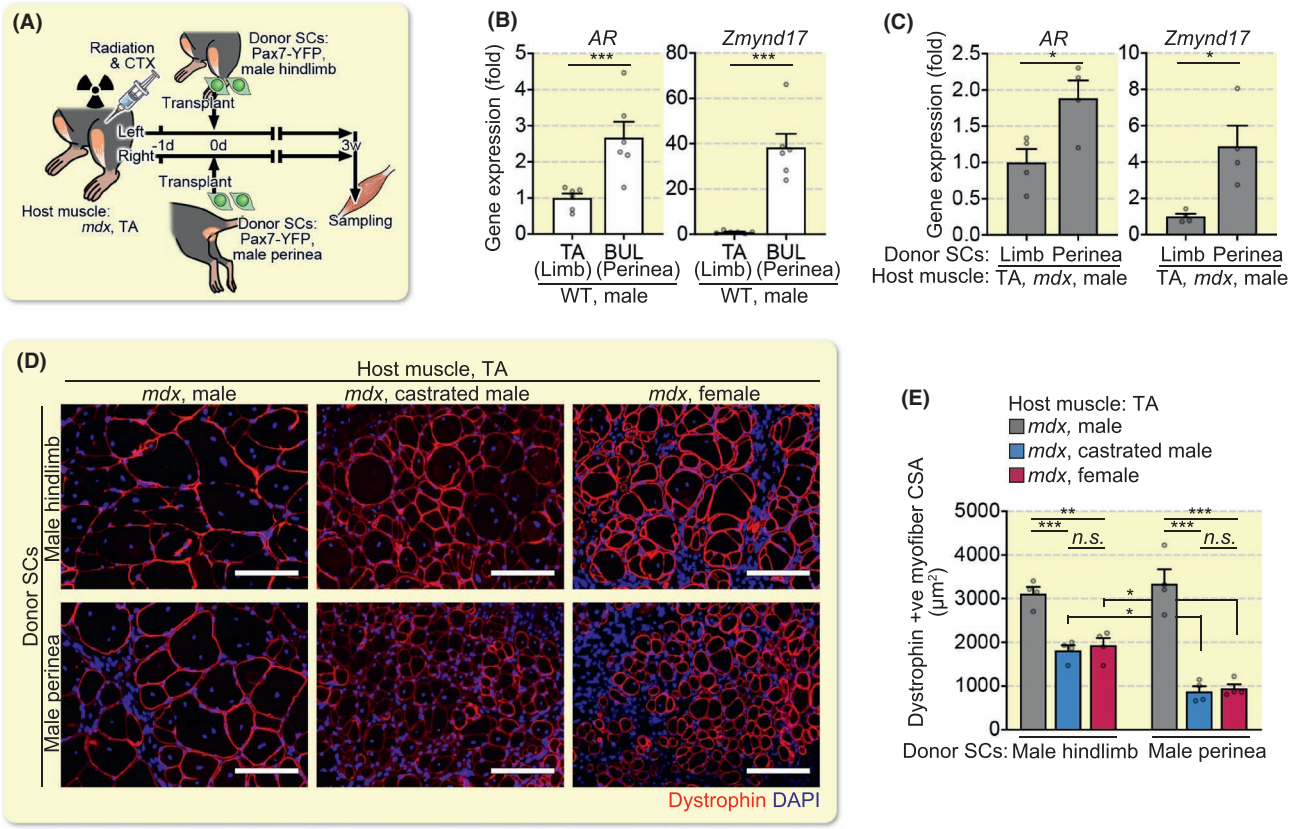

FIGURE 6 Positional identities in ectopically engrafted satellite cell-derived myofibers. (A) Schematic illustration of engraftment. TA (Host: *mdx* mice) was irradiated and pre-injured with a CTX injection. Satellite cells from the limb muscle or perineal muscle (Donor: Pax7-YFP mice) were engrafted into the TA. (B) qPCR analysis of gene expression in TA and BUL (n = 6 mice each). (C) qPCR analysis of gene expression in the engrafted TA (n = 4 mice each). (D) Representative immunohistochemical image of transverse sections of TA for dystrophin. Scale bars, 100 μm. (E) Mean CSA of the 50 largest dystrophin-positive myofibers in a section (n = 4 mice each). Two-way ANOVA results were as follow. Donor SCs, **. Host mice, ***. Interaction, **. All error bars show the SEM. *$P < .05$, **$P < .01$, ***$P < .001$. BUL, bulbospongiosus; TA, tibialis anterior

4 | DISCUSSION

During muscle development, there are distinct genetic networks in myogenic progenitors between head and limb muscles.[7–9] In adult mice, the head muscle has been reported to poorly regenerate in response to an acute muscle injury compared to the regeneration in the limb muscle.[30] In the present study, we further examined the long-term effect of a muscle injury induced by a CTX injection on head and limb muscles. Muscle mass of the head was fully recovered to that of the basal level 40 weeks after injury, whereas limb muscle took only 2 weeks to recover, and its muscle mass was gradually increased up to 40 weeks post-injury. This overgrowth alteration of limb muscles was also observed in *mdx* mice, where muscles underwent a cycle of degeneration and regeneration. It is possible that the head muscles may be mildly injured in *mdx* mice, compared with those of limb muscles, probably as result of the overexpression and correct membrane localization of utrophin protein in head muscles as previously reported.[31,32] We also found that the atrophic response of muscles was different among body regions in cancer cachexia. In this model, limb muscles except SOL were affected, while head muscles were spared despite a similar fibre-type composition between limb muscles and head muscles (mainly type IIx and IIb bases except SOL[33]). Therefore, our results indicate that regenerative potential and atrophic responses are both remarkably diverse between the head and limb muscles. Although it has been reported that the molecular signatures of satellite cells from the head and limb are different,[10,15–17,34] the mechanism underlying this diversity remains unclear. However, it may be, in part, caused by the differences in the function and number of satellite cells between the head and limb muscles: the head muscle contains a lower number of satellite cells compared to that in the limb muscles, while head satellite cells tend to maintain a longer proliferative state.[16] Satellite cells in the pharyngeal muscle of the head, but not in the limb muscle, constitutively undergo proliferation, contributing to a myonuclear turnover under basal conditions.[17] It is well accepted that the number of satellite cells declines in limb muscles with age,[35,36] but this may not be a universal phenomenon in

aged muscles since the number of satellite cells almost doubled in the head of aged mice.[16] Collectively, head and limb muscles have developmentally and functionally distinct properties in regeneration abilities and atrophic responses, which may be involved in the heterogeneity of the satellite cell population among muscles.

In mouse embryonic myogenesis, perineal muscles develop from the ventral muscle mass of hind limbs.[37] Even though the perineal and hind-limb muscles are both derived from somites, we showed that, in castrated adult mice, perineal muscles are highly influenced by sex hormones, as reported in previous studies.[25-27,38] We further found that the positional identities of satellite cells were robustly preserved in the ectopically engrafted satellite cell-derived muscles in the castrated model. It should be noted that the positional identities include not only gene expression profiles but also sex hormonal sensitivities. Since the satellite cell-based regenerative medicine shows potential in intractable muscular diseases, we may need to consider the robustness of positional identities when developing efficient stem cell therapies.

In conclusion, we described distinct patterns of muscle regeneration and atrophy, which were not only based on the embryonic origin but also the body region specificity. Our study might have had a possible limitation: we did not restrict regionally specific muscle activities such as mastication activity, which is crucial to food consumption and, therefore, might have influenced the features of muscle atrophy and regeneration. However, given that clinical observations reveal a body region–specific pathology in patients with muscular dystrophy, this study will expand our knowledge of the skeletal muscle diversity and provide new insights into the aetiology of muscle diseases as well as novel therapeutic strategies for muscle weakness.

ACKNOWLEDGEMENTS

This work was supported by the Japan Agency for Medical Research and Development (AMED, JP16bm0704010, JP18ek0109383 and JP19bm0704036), and Grants-in-Aid for Scientific Research KAKENHI (18H03193, 18K17857, 20K21763 and 20K19711). This work was also supported, in part, by the Takeda Science Foundation.

CONFLICT OF INTEREST

The authors declare that they have no competing interests.

AUTHOR CONTRIBUTIONS

KY designed and performed the experiments, analysed the data and wrote the manuscript. YK, DS, and YT performed the experiments and analysed the data. YO conceived the project, designed and performed the experiments, analysed the data, assembled the input data and wrote the manuscript. All authors discussed the results and their implications and commented on the manuscript.

ORCID

Yusuke Ono https://orcid.org/0000-0002-4802-7507

REFERENCES

1. Schiaffino S, Reggiani C. Fiber types in mammalian skeletal muscles. *Physiol Rev*. 2011;91(4):1447-1531.
2. Uchitomi R, Hatazawa Y, Senoo N, et al. Metabolomic Analysis of Skeletal Muscle in Aged Mice. *Sci Rep*. 2019;9(1):10425.
3. Mauro A. Satellite cell of skeletal muscle fibers. *J Biophys Biochem Cytol*. 1961;9:493-495.
4. Morgan JE, Zammit PS. Direct effects of the pathogenic mutation on satellite cell function in muscular dystrophy. *Exp Cell Res*. 2010;316(18):3100-3108.
5. Randolph ME, Pavlath GK. A muscle stem cell for every muscle: variability of satellite cell biology among different muscle groups. *Front Aging Neurosci*. 2015;7:190.
6. Emery AE. The muscular dystrophies. *BMJ*. 1998;317(7164):991-995.
7. Diogo R, Kelly RG, Christiaen L, et al. A new heart for a new head in vertebrate cardiopharyngeal evolution. *Nature*. 2015;520(7548):466-473.
8. Sambasivan R, Kuratani S, Tajbakhsh S. An eye on the head: the development and evolution of craniofacial muscles. *Development*. 2011;138(12):2401-2415.
9. Schubert FR, Singh AJ, Afoyalan O, Kioussi C, Dietrich S. To roll the eyes and snap a bite - function, development and evolution of craniofacial muscles. *Semin Cell Dev Biol*. 2019;91:31-44.
10. Harel I, Nathan E, Tirosh-Finkel L, et al. Distinct origins and genetic programs of head muscle satellite cells. *Dev Cell*. 2009;16(6):822-832.
11. Kelly RG, Jerome-Majewska LA, Papaioannou VE. The del22q11.2 candidate gene Tbx1 regulates branchiomeric myogenesis. *Hum Mol Genet*. 2004;13(22):2829-2840.
12. Tajbakhsh S, Rocancourt D, Cossu G, Buckingham M. Redefining the genetic hierarchies controlling skeletal myogenesis: Pax-3 and Myf-5 act upstream of MyoD. *Cell*. 1997;89(1):127-138.
13. Relaix F, Rocancourt D, Mansouri A, Buckingham M. A Pax3/Pax7-dependent population of skeletal muscle progenitor cells. *Nature*. 2005;435(7044):948-953.
14. Shih HP, Gross MK, Kioussi C. Cranial muscle defects of Pitx2 mutants result from specification defects in the first branchial arch. *Proc Natl Acad Sci USA*. 2007;104(14):5907-5912.
15. Sambasivan R, Gayraud-Morel B, Dumas G, et al. Distinct regulatory cascades govern extraocular and pharyngeal arch muscle progenitor cell fates. *Dev Cell*. 2009;16(6):810-821.
16. Ono Y, Boldrin L, Knopp P, Morgan JE, Zammit PS. Muscle satellite cells are a functionally heterogeneous population in both somite-derived and branchiomeric muscles. *Dev Biol*. 2010;337(1):29-41.
17. Randolph ME, Phillips BL, Choo HJ, Vest KE, Vera Y, Pavlath GK. Pharyngeal satellite cells undergo myogenesis under basal conditions and are required for pharyngeal muscle maintenance. *Stem Cells*. 2015;33(12):3581-3595.
18. Noden DM, Francis-West P. The differentiation and morphogenesis of craniofacial muscles. *Dev Dyn*. 2006;235(5):1194-1218.
19. Collins CA, Olsen I, Zammit PS, et al. Stem cell function, self-renewal, and behavioral heterogeneity of cells from the adult muscle satellite cell niche. *Cell*. 2005;122(2):289-301.

20. Kitajima Y, Ono Y. Visualization of PAX7 protein dynamics in muscle satellite cells in a YFP knock-in-mouse line. *Skelet Muscle*. 2018;8(1):26.
21. Ono Y, Urata Y, Goto S, et al. Muscle stem cell fate is controlled by the cell-polarity protein Scrib. *Cell Rep*. 2015;10(7):1135-1148.
22. Yucel N, Chang AC, Day JW, Rosenthal N, Blau HM. Humanizing the mdx mouse model of DMD: the long and the short of it. *NPJ Regen Med*. 2018;3:4.
23. McPherron AC, Lawler AM, Lee SJ. Regulation of skeletal muscle mass in mice by a new TGF-beta superfamily member. *Nature*. 1997;387(6628):83-90.
24. Bodine SC, Latres E, Baumhueter S, et al. Identification of ubiquitin ligases required for skeletal muscle atrophy. *Science*. 2001;294(5547):1704-1708.
25. Chambon C, Duteil D, Vignaud A, et al. Myocytic androgen receptor controls the strength but not the mass of limb muscles. *Proc Natl Acad Sci USA*. 2010;107(32):14327-14332.
26. Monks DA, Holmes MM. Androgen receptors and muscle: a key mechanism underlying life history trade-offs. *J Comp Physiol B*. 2018;204(1):51-60.
27. Yoshioka K, Tomohiro M, Kodai N, et al. Castration-induced pelvic floor muscle specific atrophy and the effect of voluntary wheel-running exercise. *J Jpn Phys Ther Assoc*. 2020;11714: 1–7.
28. Fujita R, Yoshioka K, Seko D, et al. Zmynd17 controls muscle mitochondrial quality and whole-body metabolism. *FASEB J*. 2018;32(9):5012-5025.
29. Yoshioka K, Fujita R, Seko D, Suematsu T, Miura S, Ono Y. Distinct roles of Zmynd17 and PGC1alpha in mitochondrial quality control and biogenesis in skeletal muscle. *Front Cell Develop Biol*. 2019;7:330.
30. Pavlath GK, Thaloor D, Rando TA, Cheong M, English AW, Zheng B. Heterogeneity among muscle precursor cells in adult skeletal muscles with differing regenerative capacities. *Dev Dyn*. 1998;212(4):495-508.
31. Muller J, Vayssiere N, Royuela M, et al. Comparative evolution of muscular dystrophy in diaphragm, gastrocnemius and masseter muscles from old male mdx mice. *J Muscle Res Cell Motil*. 2001;22(2):133-139.
32. Marques MJ, Ferretti R, Vomero VU, Minatel E, Neto HS. Intrinsic laryngeal muscles are spared from myonecrosis in the mdx mouse model of Duchenne muscular dystrophy. *Muscle Nerve*. 2007;35(3):349-353.
33. Mathewson MA, Chapman MA, Hentzen ER, Friden J, Lieber RL. Anatomical, architectural, and biochemical diversity of the murine forelimb muscles. *J Anat*. 2012;221(5):443-451.
34. Hernando-Herraez I, Evano B, Stubbs T, et al. Ageing affects DNA methylation drift and transcriptional cell-to-cell variability in mouse muscle stem cells. *Nat Commun*. 2019;10(1):4361.
35. Chakkalakal JV, Jones KM, Basson MA, Brack AS. The aged niche disrupts muscle stem cell quiescence. *Nature*. 2012;490(7420):355-360.
36. Sousa-Victor P, Gutarra S, García-Prat L, et al. Geriatric muscle stem cells switch reversible quiescence into senescence. *Nature*. 2014;506(7488):316-321.
37. Valasek P, Evans DJ, Maina F, Grim M, Patel K. A dual fate of the hindlimb muscle mass: cloacal/perineal musculature develops from leg muscle cells. *Development*. 2005;132(3):447-458.
38. Monks DA, Holmes MM. Androgen receptors and muscle: a key mechanism underlying life history trade-offs. *J Comp Physiol A Neuroethol Sens Neural Behav Physiol*. 2018;204(1):51-60.

How to cite this article: Yoshioka K, Kitajima Y, Seko D, Tsuchiya Y, Ono Y. The body region specificity in murine models of muscle regeneration and atrophy. *Acta Physiol*. 2021;231:e13553. https://doi.org/10.1111/apha.13553